A Comprehensive Study on the Influence of Scale and Draft Variations on Form Factor Using a Combined EFD/CFD Approach

Technology and Science for the Ships of the Future
V. Crupi and V. Bucci (Eds.)

doi:10.3233/PMST250043

A Comprehensive Study on the Influence of Scale and Draft Variations on Form Factor Using a Combined EFD/CFD Approach

Minas ARGYROS[a], Simone MANCINI[b], Kadir BURAK KORKMAZ[c], Arash ESLAMDOOST[d]
[a]*Department of Hydro and Aerodynamics, FORCE Technology, Hjortekærsvej 99, Copenhagen, 2800, Denmark*
[b]*Department of Industrial Engineering, University of Naples Federico II, Via Claudio 21, Napoli NA, 80125, Italy*
[c]*RISE Research Institutes of Sweden, Chalmers Tvärgata 10, Göteborg, Box 24001, Se-400 22, Sweden*
[d]*Department of Mechanics and Maritime Sciences, Chalmers University of Technology, Chalmersplatsen 4, Gothenburg, 412 96, Sweden*

Abstract. In recent years, extensive research has been conducted on predicting a ship's form factor and the associated scale effects, as the accuracy of these estimates has been questioned. This study examines the differences between model and full-scale CFD-based form factor calculations using a newly developed approach known as the 2-k method. This method enhances the precision of form factor estimation by applying full-scale computations, particularly in scenarios involving stern flow separation. The study evaluates three benchmark hulls and two bulk carriers, revealing a strong dependence of the form factor on grid resolution due to variations in scale factors. The results align well with findings from existing literature. Additionally, a systematic variation of transom submergence demonstrates consistency in form factor predictions at both model and full scale. Through a comprehensive analysis of scale and draft variations, the study confirms that the 2-k method is a robust and reliable approach, capable of accurately predicting the form factor even in the presence of recirculating flow behind a submerged transom.

Keywords. Computational Fluid Dynamics, Scale effects, Draft effects, Form Factor, 2-*k* method

1. Introduction

During the preliminary design phase of a vessel, it is paramount that the designer acquire an accurate estimation of the vessel's performance. This precision in prediction is vital to ensure compliance with stipulated requirements, minimize overall construction and operational costs, and facilitate the design of an environmentally efficient ship. The progressively stringent regulations imposed by international governing authorities,

aimed at fostering sustainability and environmental consciousness, underscore the necessity and inevitability of eco-efficiency within the maritime sector.

In accordance with established practices and extensive knowledge, towing tank testing remains a fundamental method for evaluating a ship's performance. Hydrodynamic tests involve scaled model versions of actual vessels and are conducted in towing tanks. This traditional testing approach has led to the acquisition of extensive experience and knowledge in ship hydrodynamics, including databases of ship models, measurements, and statistical data. With the accumulation of invaluable information on ship hydrodynamics, standardized procedures have been devised to perform towing tank tests. The main responsible for organizing and publishing these procedures is the International Towing Tank Conference (ITTC).

It is a fact that CFD provides advantages, but it also conceals drawbacks. The main advantage of CFD is its ability to run full-scale simulations, which reduces uncertainties in the extrapolation from model to full-scale. Additionally, valuable flow information can be obtained from a CFD simulation, making it a viable positive choice. However, it should be noted that the CFD is affected by uncertainties and modeling errors. These errors occur because flow physics is simulated by using simplified models, such as the use of wall functions to represent turbulence effects inside the boundary layer [13] or the lack of accurate models to represent surface roughness.

In addition to the experimental methods for the determination of the form factor, such as Hughes [4] and Prohaska [14] methods, recently research studies have presented that a combination of CFD computations and Experimental Fluid Dynamics (EFD) can handle scale effects and draft variations and estimate the form factor with a combined EFD & CFD method. This method is called the two form factor method [10, 9]. The main idea behind it is that combining CFD and EFD at their strong points can result in a more accurate estimation of the form factor and consequently in power prediction. Additionally, a potential alternative or complementary method to the Prohaska approach is to use double-body Reynolds-Averaged Navier- Stokes (RANS) computations, which are also used in the present study. Recently, [15] have implemented a similar approach for form factor estimation combining EFD and CFD methods in order to improve the full-scale resistance prediction.

In this study, a systematic analysis of scale effects, as well as variations in roughness and draft, is carried out by comparing the numerically calculated form factors with available experimental data. The combined EFD&CFD form-factor calculation approach and its improvement (the 2-k form factor) proposed by [10] and [9] was applied to calculate the form factor and assess possible improvement in the extrapolation procedure from model to full-scale (1978 ITTC Performance Prediction Method [6]).

2. Theoretical Background

A brief description of the governing equations, which describe the CFD simulations, is presented. Additionally, in this section, the experimental determination of the form factor and the 2-*k* method are shown.

2.1. Governing equations

The governing equations of a fluid flow are the so-called continuity and the Navier-Stokes equations. These equations represent a system of nonlinear partial differential

equations originating from the fundamental principles of mass and momentum conservation. Cartesian tensors are used in the continuity and Navier-Stokes equations to make them more compact. This means that the vector components are represented by one index, and the tensor components by two indices.

Moreover, the equations are made more compact due to Einstein's summation notation. Therefore, the continuity equation, Equation 1, and the Reynolds-averaged Navier-Stokes equation, Equation 2, for an incompressible Newtonian fluid are

$$\frac{\partial u_i}{\partial x_i} = 0 \tag{1}$$

$$\frac{\partial u_i}{\partial t} + u_j \frac{\partial u_i}{\partial x_j} = -\frac{1}{\rho}\frac{\partial p}{\partial x_i} + F_i + \nu \frac{\partial^2 u_i}{\partial x_j \partial x_j} \tag{2}$$

where i and j are the abscissa and ordinate, respectively, u_i represents the velocity components, x_i are the three coordinate components, F_i are the external forces, and ν is the kinematic viscosity.

2.2. Experimental and empirical determination of form factor

The determination of the form factor is usually based on three different approaches [18]. To derive a first estimate of the form factor, [18] introduced the following empirical expression (Equation 3).

$$k = -0.095 + 25.6 \cdot \frac{C_B}{(L/B)^2\sqrt{B/T}}. \tag{3}$$

Equation 3 is only used in conjunction with the [5] formula, see Equation 4.

$$C_F = \frac{0.075}{(\log Re - 2)^2} \tag{4}$$

The second widespread way to define form factor is by running the model at low speed, where wave making resistance becomes negligible, and thus the friction is the only contributor in total resistance [4]. In this approach, the frictional resistance coefficient C_F is calculated using the ITTC57 formula (Equation 4). The form factor can also be calculated using the formula Equation 5, where C_F was derived from CFD simulations (CFD-based form factor).

$$(1 + k) = \frac{C_F + C_{PV}}{C_F} = \frac{C_V}{C_F} \tag{5}$$

Prohaska method is the third approach to define the form factor and is considered the most common and reliable [18]. This method is applied in the present study for the systematic analysis of transom submergence. The main idea of the Prohaska method is the expression of the wave-making resistance coefficient C_W with the representation of the asymptotic expansion.

After neglecting the components of the highest order from the asymptotic expansion, the linear expression of Equation 6 arises:

$$C_{TM}/C_F = (1 + k) + a \times Fr^4/C_F. \tag{6}$$

2.3. 2.3. The two form factor (2-k) method

The recirculation region behind the transom, which is one of the challenges of the Prohaska method, is assumed to be the same for all Re numbers from model to full-scale. This leads to an under-prediction of viscous resistance at full-scale.

To address this problem, the model-scale decomposition of the viscous resistance coefficient (C_{PVM}), also known as form resistance, is introduced as shown in Equation 7 [9]

$$C_{PVM} = C'_{PVM} + C_{trM}, \tag{7}$$

where C'_{PVM} represents the proportional part to C_F based on the criteria of [4], and C_{trM} corresponds to the resistance due to the flow separation behind the transom which is not proportional to C_F. This methodology is called the two form factor (2-k) method and certain steps are needed for its application.

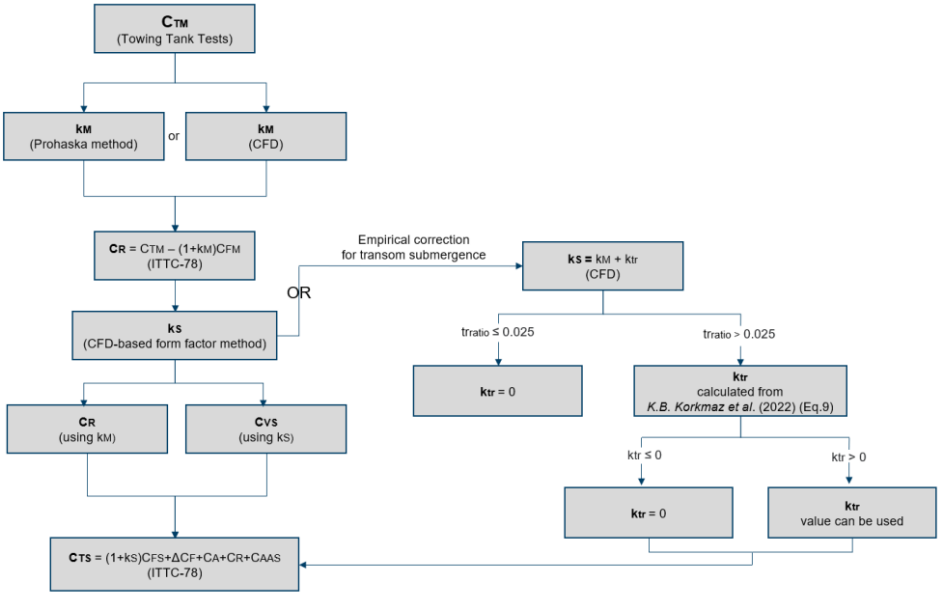

Figure 1: Flow chart of 2-k method.

An empirical correction formula, Equation 8, has been proposed by [9] through regression analysis. This formula is established to include the effect of recirculation in the wake of transom due to its submergence.

$$k_{tr} = [-0.025+tr_{ra}(1.5-2.3tr_{ra}-0.07\,LCB)]\times[-5.45+\log_{10}(\overline{Re_M})(1.415+4.32tr_{ra})-(\log_{10}(\overline{Re_M}))^2(0.081+0.55tr_{ra})] \tag{8}$$

In Equation 8, $\overline{Re_M}$ is the average Reynolds number on the model-scale and LCB is relative to $L_{PP}/2$. By comparing the k_{tr} values from CFD and the empirical correction formula Equation 8, the two methods demonstrate minor discrepancies, as shown in Section 5. Equation 9 expresses the percentage of transom submergence and is used to apply the empirical formula.

$$tr_{ra} = \frac{A_{tr}}{A_{max}} \tag{9}$$

where A_{tr} is the area of the submerged transom, A_{max} is the maximum cross-section area for a given draft and ytr is the transverse dimension of the wetted transom. Based

on [9], the lower limit for tr_{ra} is established ($tr_{ra} \leqslant 0.025$), as lower values can result in a partially wetted or dry transom flow.

3. CFD simulations setup

The computational domain and boundary conditions of the CFD simulations setup are presented, along with an illustration and commentary on the generated mesh. Additionally, the computational approaches (Double Body and Free-Surface) being used are detailed.

3.1. Computational domain, boundary conditions and mesh generation

A body-fixed reference frame $x_0y_0z_0$ is defined at the initial position of the ship's center of gravity (COG) and it follows the hull geometry's motions and its instantaneous speed. The dimensions of the computational domain and the several refinement zones are measured taking the body-fixed system into account as the origin. Figure 2 shows the side view of the computational mesh in both approaches. The generated computational domain is a rectangular box to simulate a towing tank. The dimensions of the computational field are selected depending on the scale factor of the hull in each case.

A symmetry plane is used because the flow is symmetric on both sides (starboard and portside), reducing the computational cost of the simulations to half. In addition, a refinement zone is applied to the grid to capture abrupt changes in flow, such as velocity and pressure fields. The refinement direction for the region near the geometry is consistent across the three dimensions (longitudinal, transverse, and vertical). No further refinement zones are needed as the double-body assumption does not account for the interaction with free surface. Table 1 shows the grid size of the generated meshes for the five hulls in both the numerical models on model and full scale.

Table 1. Number of cells in double body and free surface approach in both model and full-scale for all studied hulls.

Test Case	Double body method		Free surface method	
	model-scale [$\times 10^7$]	full-scale [$\times 10^7$]	model-scale [$\times 10^7$]	full-scale [$\times 10^7$]
JBC	0.565	1.002	0.982	1.318
KCS	0.544	0.997	0.912	1.265
KVLCC2	0.685	1.142	1.122	1.439
180K DWT BC	0.631	1.081	1.008	1.376
82K DWT BC	0.512	0.896	0.873	1.140

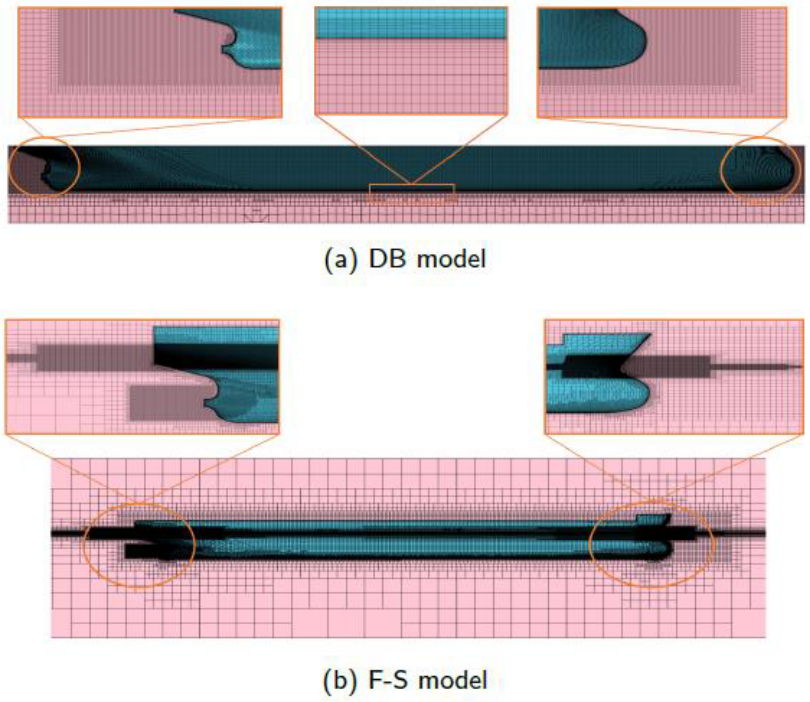

Figure 2: Representation of generated mesh with a close-up of the bow and stern for both DB and F-S numerical computations (side view - JBC).

The computational domain for all test cases and both the DB and the F-S methods in model and full-scale is composed of hexahedral orthogonal cells. The generated mesh is considered an isotropic volume mesh, where every pair of adjacent cells of the same size in the grid with n = 1.00 is transformed into $2n$ cells along each axis (X, Y and Z), resulting in a total of $2n^3$ cells. The grid generation is implemented by taking into account certain features of the flow field, which are relevant to the viscous and turbulence effects of the flow, and the frictional contribution to the total resistance of the studied hulls, as they are the decisive factors in the analysis and scope of this study. The CFD simulations have been set up using physical time equal to $55s$, maximum time steps equal to 2000 and time step (Δt) equal to $0.01s$.

3.2. Numerical models

In the following sections, the details of the two main simulation strategies are presented, specifically the Double-Body and the Free-surface approaches, showing their assumptions, limitations and advantages.

3.2.1. Double-Body approach

The *Double-Body* (DB) approach is a simulation strategy based on a specific assumption. At very low speeds, the free-surface effects are considered negligible because the wave-making resistance does not significantly contribute to the total resistance. The DB assumption is practically applied by imposing a symmetry boundary condition on the

plane representing the undisturbed free surface, therefore avoiding any free surface effect in the CFD computations. [20] verifies that the DB assumption is suitable and efficient for low speeds (i.e. $Fr < 0.142$), where hull-generated waves are negligible. The final predicted results closely approximate the experimental towing tank data. The computational cost of a DB simulation is significantly less than other approaches since the free-surface is neglected and a steady solver is usually implemented.

3.2.2. Free-surface model including Dynamic Fluid Body Interaction

For a more accurate prediction of the flow around a hull, free surface computation is crucial, especially at higher Froude numbers, since the generated waves have a significant contribution to the total ship resistance. Besides the importance of capturing hull-generated waves, in the context of this work, free surface simulations were carried out to capture the flow behind the submerged transom to study the impact of the wetted transom on the form factor. The Volume of Fluid (VoF) technique is employed in order to model the fluid interface of a free surface, using the approach of High-Resolution Interface Capturing (HRIC). The two fluid phases, namely water and air, are determined by their respective phase volume fraction (α).

α is defined as a numerical value between zero and one, and is determined by the following calculation:

$$\frac{\partial \alpha}{\partial t} + \nabla \cdot (\alpha u) = 0 \tag{10}$$

Fluid density and viscosity are calculated as:

$$\rho = \alpha \cdot \rho_w + (1 - \alpha) \cdot \rho_\alpha \tag{11}$$

$$\mu = \alpha \cdot \mu_w + (1 - \alpha) \cdot \mu_\alpha \tag{12}$$

where subscripts α and w indicate air and water, respectively. The fluid-ship interaction is considered a decisive factor for the assessment of resistance. Through considering the aforementioned interaction in the simulations, sinkage and trim of the hull are obtained. Since the hull sinkage and trim are of interest in this study, only two fundamental Degrees of Freedom (DoF) of the hull are taken into account in still water. To this end, the Dynamic Fluid-Body Interaction (DFBI) method is employed ([16]). Finally, an implicit-unsteady solver is used in conjunction with the VOF-HRIC and the FBI approaches.

4. Verification and Validation (V&V) study

A method for evaluating accuracy in numerical modeling is through verification and validation (VV). The verification is defined as a process for assessing the simulation numerical uncertainty while the validation is defined as a process for assessing the modelling uncertainty by comparing the results obtained from the numerical simulations with experimental or analytical data to determine the comparison errors. The verification process assesses the iterative and parameter convergence studies based on the Generalized Richardson extrapolation applied to the multiple solutions approach. Several methods were developed to practically estimate the numerical uncertainty such as the Grid Convergence Index, the Convergence Factor and the Factor of Safety.

The simulation's numerical uncertainty (U_{SN}) consists mainly of four uncertainties, as shown in Equation 13.

$$U_{SN} = \sqrt{U_G^2 + U_I^2 + U_T^2 + U_P^2} \tag{13}$$

where U_G is the grid uncertainty, U_I is the iterative uncertainty, U_T is the time-step uncertainty, and U_P is the uncertainty related to other parameters. For typical simulations in the marine hydrodynamics field (e.g. resistance and self-propulsion simulations), the computational grid may be considered the primary source of uncertainty [19, 17].

As mentioned above, the validation of a numerical simulation is achieved by comparing the computed value with the experimentally measured one. The validation assesses the modelling uncertainty (U_{SM}) by using experimental data and the estimation of the sign and magnitude of the modelling error δ_{SM}. In the validation process, two parameters are included, which are the validation comparison error (Equation 14) and the validation uncertainty (Equation 15)

$$E = D - S = \delta_D - (\delta_{SM} + \delta_{SN}) \tag{14}$$

$$U_V^2 = U_{SN}^2 + U_D^2 \tag{15}$$

where E is the comparison error, S is the solution of simulation, D is the solution from experiment, δ_D is the difference between experimental and real data, δ_{SN} is the simulation error, U_D is the uncertainty of the data from the experiments, and U_V validation uncertainty.

Finally, after the determination of the validation comparison error and the validation uncertainty, the validation result can be split in two different ways:

- For $|E| > U_V$, all errors in both D and S are greater than U_V and therefore validation is not achieved for this validation uncertainty level. The magnitude of the validation uncertainty gives the level of confidence in the CFD model.
- For $|E| < U_V$, all errors in both D and S are smaller than UV and thus validation is achieved in the U_V interval [7]. When $|E| \ll U_{val}$, the δ_{SM} indicates that the numerical models implemented in the simulation need to be improved.

In addition to the grid refinement sensitivity analysis, the grid uncertainty has been investigated for both MS and FS, as well as both turbulence models. The depicted results in 3 are related to JBC test case.

5. Results

The results of scale and daft sensitivity analyzes are presented in this section.

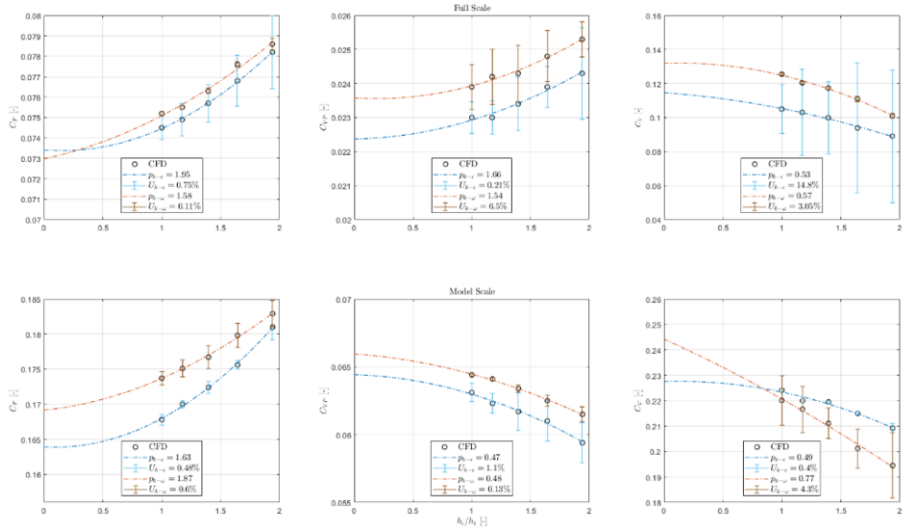

Figure 3: Convergence of C_F, C_{PV} and C_V with the grid refinement ratio for JBC. Fits obtained from the data with $1 \leqslant h_i/h_1 \leqslant 2$ for k - ω SST and realizable k - ϵ models in MS and FS.

5.1. Scale effect

A systematic analysis of different scaling factors is implemented. Specifically, the effect of systematic variation of the scale factor of JBC, KCS and KVLCC2 on the C_F, C_{PV} and C_V is studied. In addition to the model and the full-scale, six additional scale factors ($\lambda_i = \lambda/16, \lambda/8, \lambda/4, \lambda/3, \lambda/2$) have also been investigated.

Figure 4 on top depicts the comparison between the ITTC57 friction line and the CFD results for JBC,KCS, and KVLCC2.

From our CFD computations, the frictional resistance coefficient includes additional effects such as curvature and transverse flows, reflecting form resistance rather than pure friction. As a result, CFD-derived CF values are typically higher compared to theoretical friction lines designed for zero pressure gradient scenarios. The ITTC-57 line, however, is not a pure friction line but an engineering approximation, adjusted for specific purposes, and it shows significantly larger values at model-scale

Reynolds numbers. At higher Reynolds numbers (beyond $Re \approx 1 \times 10^8$), the CF values from CFD and the ITTC-57 line become nearly parallel, indicating a closer approximation to pure friction behavior. The second row of the plots shown in Figure 4 represents the correlation between the form factor and Re (scale factor). The plots also include ITTC57-based and numerical-based friction line EFD data. The model-scale ITTC57-based EFD data have been derived from [3] for JBC and [12] for KCS and KVLCC2. The numerical-based friction line EFD form factor was obtained by [8], which has been expressed as a cubic polynomial in logarithmic scales. The form factor values were calculated using Equation 5, where CF was derived from CFD simulations (CFD-based form factor) or calculated using the ITTC57 friction line (ITTC57-based form factor).

The ITTC57-based form factors show an increasing trend in all test cases, which tend to converge to a constant value when the scaling factor approaches full-scale. On the other hand, CFD-based form factors have a scant impact from scale effect.

The comparison between EFD, ITTC57-based, and CFD-based form factors for each hull is presented below:

- **JBC**: CFD-based formfactors are periodically increasing by 1.8%from model to full-scale, while formfactors extracted from the friction line ITTC57 perform a slight increase of 3 % from model to full-scale. Their differences from the EFD values are 4.1 and 5.2, respectively.
- **KCS**: The greatest discrepancy between the extracted CFD formfactors and the numerical-based EFD value is observed in full-scale and it is equal to 1.4%, while the biggest difference between the ITTC57 friction line and the ITTC57-based EFD form factor is 4%.
- **KVLCC2**: CFD results show a constant trend along the range of Re numbers, except for the case of the model scale, which has a difference of 2.5 % from the rest of the CFD form factor results. ITTC57 friction line form factor results show a linear increment as in the other two test cases of 5.2 % from model to full-scale.

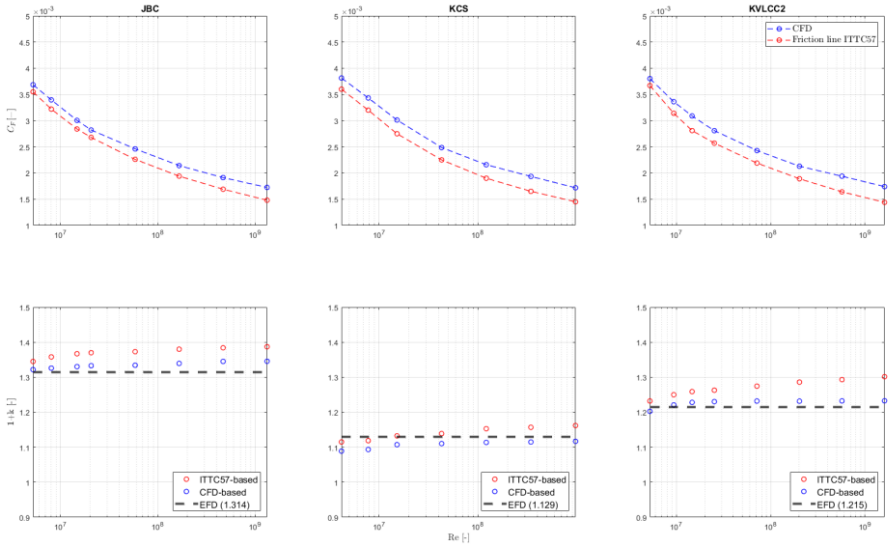

Figure 4: Correlation between ITTC57 friction line and CFD frictional resistance coefficient (top), and form factor variation (bottom) through scales.

The flow behind the transom of the three aforementioned test cases has been studied for both MS and FS in the scantling draft, excluding the roughness effect (hydrodynamically smooth surface). Figure 5 shows the normalized axial velocity (u/U) distribution, as well as the in-plane streamlines, on a plane behind the transom ($x/L_{PP} = -0.05$) obtained from the MS and FS simulations including the free surface. The lower limit of the normalized velocity has been set to -0.1 to show the forwardmoving flow due to the flow separation. These plots reveal a discrepancy between the model and the full-scale axial velocity distribution as well as the effect of the bilge vortex in the propeller plane and the impact of the transom submergence. The model-scale wake is slightly wider and more pronounced relative to the full-scale for all test cases. In the case of KVLCC2, the discrepancy of the wake between model-scale and full-scale is more visible if one

observes the streamlines in the transom area, as well as the bigger diameter of the bilge vortex.

5.2. Transom submergence effect

Variation in transom submergence significantly affects total resistance and constitutes an important part of the 2-k method.

Therefore, in a systematic variation of the draft, the effect of transom submergence on the local flow behind the transom is studied in the current work. The benchmark hulls including JBC, KCS, KVLCC2, and the two commercial hulls have been chosen for this systematic analysis. The two commercial hulls are selected since model test results are available from the FORCE Technology's database [1], [2].

Comparison of y-intercept between model-scale and full-scale shows that broader range of C_{Tm}/C_{Fm} values is observed in full-scale than in model-scale for 180K DWT BC and 82K DWT BC among the studied drafts. In case of JBC, asymptotic values in full-scale cover a narrower range of the C_{Tm}/C_{Fm} ratio.

Table 2 shows the results on the form factor prediction of all the test cases in both the model and the full-scale. The comparison errors of the CFD and EFD form factors shown in Table 2 are obtained through Equation 16.

$$\Delta k = \frac{k_{CFD} - k_{EFD}}{k_{CFD}} \times 100\ [\%] \tag{16}$$

Table 2 presents the discrepancies between the CFD-based form factor estimation and the EFD results. The comparison errors for most test cases are less than 5 %, which indicates the reliability of the CFD-based form factor estimations. Based on the results in Table 2, the 2-k method gives lower discrepancy of form factor values comparing with the ones provided by EFD for KVLCC2 and 180K DWT BC. For the other test cases, the form factor estimation obtained by the 2-k method has a discrepancy with the EFD data similar to the discrepancy between the EFD data and the exact CFD results in model scale and full scale.

Figure 6 shows the form factor of JBC, KCS, and KVLCC2, as well as the two commercial vessels for different transom submergence. The results are obtained from CFD-based model-scale, full-scale simulations, and full-scale simulations using the transom submergence correction formula. The resulting form factors are based on CFD-based C_F. A difference of less than 5.0 % is observed for all test cases except KCS. In this case, the discrepancy between CFD-based estimate in model and full-scale with the form factors extracted using the empirical formula of the 2-k method, Equation 8, is 5.1 % and 6.7 % for drafts 16.0 and 17.0 m, respectively. KCS is the only container ship studied in this analysis, whereas the other test cases include three bulk carriers and a tanker. Specifically, the shape of the KCS hull, particularly its stern, differs compared to the rest of the test cases, as it has a larger wetted transom area. This leads to more intense recirculation and turbulence in the wake of the transom, resulting in a more significant impact on form resistance, that is, C_{VP}. Hence, C_{VP} is increasing sharply, while C_F remains relatively similar resulting in increased form factor. and the form factor in full-scale CFD simulations. Generally, the formfactor is sensitive to the wetted transom area and larger transom areas result in a higher formfactor, indicating greater flow separation and energy loss in the wake of the ship and thus higher resistance.

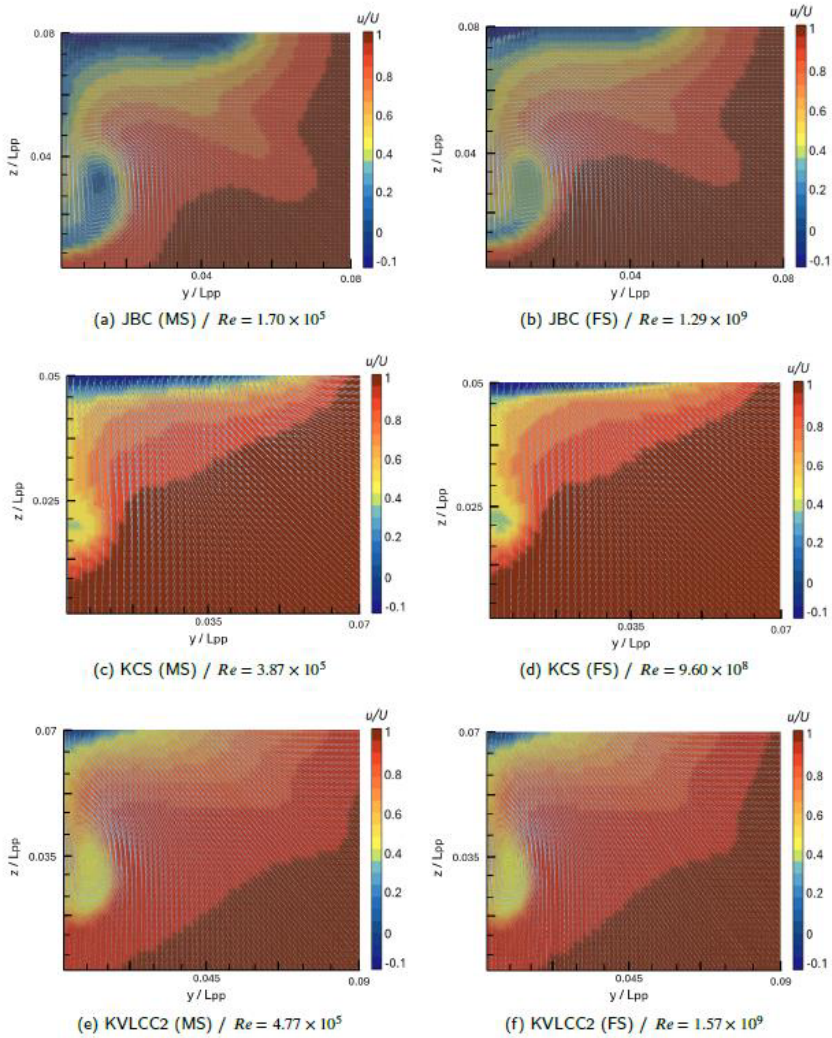

Figure 5: Normalized axial velocity of the wake with in-plane arrows indicating flow direction for the scantling draft at $x/L_{PP} = -0.05$ and $Fn = 0.1$ in both MS and FS (F-S, $k - \omega$ model, AHR = 0).

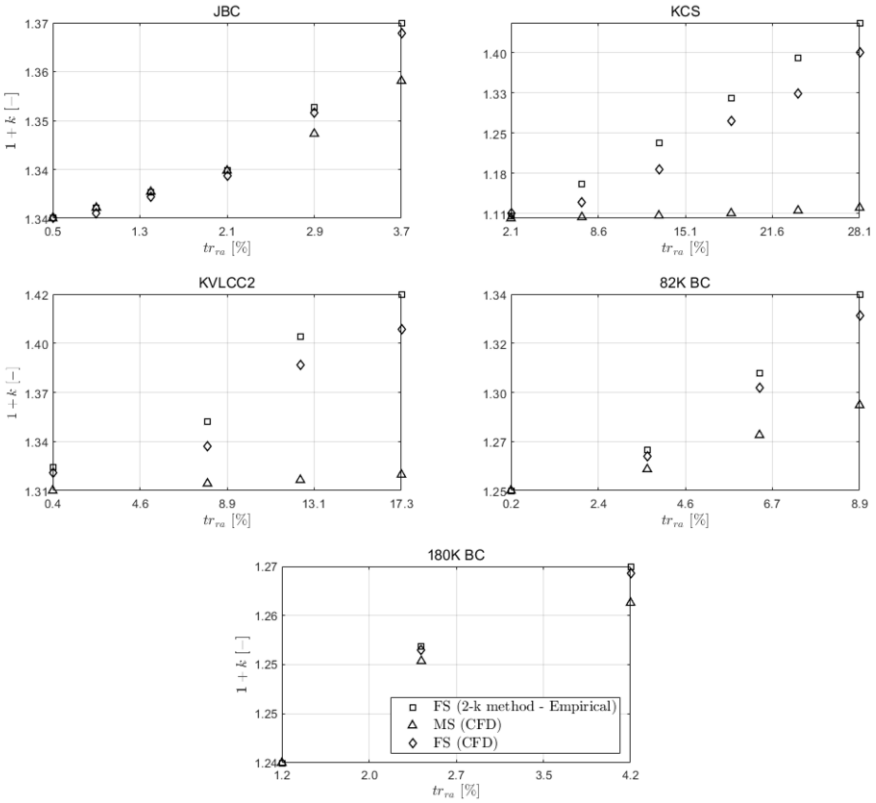

Figure 6: Sensitivity of 1+k under transom submergence variation for all test cases.

Table 2. Comparison of 1+k results with data from the literature in model-scale and full-scale using CFD-based frictional resistance and the DB model. All results correspond to scantling draft.

Test Case	CFD		2-k method	EFD	CFD vs EFD		CFD MS vs CFD FS	2-k vs EFD
	MS	FS			MS	FS		
JBC	1.312	1.322	1.335	1.314 [3]	0.23 %	0.61 %	3.92 %	1.50 %
KCS	1.090	1.131	1.109	1.129 [11]	3.45 %	0.18 %	3.63 %	1.77 %
KVLCC2	1.257	1.268	1.234	1.215 [11]	2.38 %	3.23 %	0.87 %	1.20 %
180K DWT BC	1.231	1.202	1.195	1.182 [1]	2.92 %	1.66 %	2.36 %	1.09 %
82K DWT BC	1.252	1.247	1.252	1.262 [1]	0.79 %	0.12 %	0.40 %	0.82 %

6. Conclusions and Future Work

This paper presents a systematic analysis of CFD-based form factor predictions applying the 2-*k* method, when scale effects, surface roughness and draft variations are considered. CFD simulations have been performed on both the model-scale and the full-scale for five reference hulls and two commercial hulls, using k – ω SST and realizable k – ϵ turbulence models.

The effect of the recirculating water region behind the submerged transom is also studied. The following conclusions for the two analyses are presented:

- Scaling variation has been shown to have an insignificant impact on the form factor for CFD-based form factor prediction. On the other hand, a discrepancy of 5-7 % in the form factor is observed between the model scale and the full scale when the ITTC-57 friction line is used. It is also shown that the CFD-based form factors at different scales agree fairly well with the results obtained from the EFD-based procedure, following the Prohaska method, for all test cases.
- The systematic study of the effect of transom submergence on the form factor reveals the impact of the wetted transom on the form factor when the draft increases, since transom submergence results in a larger recirculating water region behind the transom, which affects the ratio C_T/C_F in a range of 4-10 % for smooth hull surface and 9-16 % for rough hull surface. The results indicate that the form factor has a linear dependence on the wetted-transom ratio for all studied hulls.

This study highlights the strengths, limitations, and uncertainties of the CFD computations and EFD data. It shows that the CFD-based form factor estimation in both model and full-scale is reliable when compared to EFD data. Despite some weaknesses, the analysis confirms the dependence of the form factor on scale effects, hull roughness, and draft variations, supporting the 2-k approach as a comprehensive method. More studies could be conducted with more test cases, especially hulls with different transom configurations and drafts for which EFD data are available. Moreover, additional simulations incorporating higher AHR values are considered essential to capture a broader range of operational conditions and better understand the nonlinear effects of roughness.

References

[1] FORCE, T., 2021a. 121-29152 energy saving devices analysis for a 180k dwt bulk carrier.
[2] FORCE, T., 2021b. 121-30654 energy saving devices analysis for a 82k dwt bulk carrier.
[3] Hino, T., Stern, F., Larsson, L., M., V., Hirata, N., Kim, J., 2015. Numerical Ship Hydrodynamics, An Assessment of the Tokyo 2015 Workshop. Volume 94, Springer. URL: https://link.springer.com/book/10.1007/978-3-030-47572-7. iSBN: 978-3-030-47571-0.
[4] Hughes, G., 1954. Friction and form resistance in turbulent flow, and a proposed formulation for use in model and ship correlation. R.I.N.A. 96 .
[5] ITTC, 1957. Subjects 2 and 4 skin friction and turbulence stimulation .
[6] ITTC, 1978. Report of performance committee URL: https://www.marin.nl/en/research/free-resources/verification-and-validation/verification-tools.
[7] ITTC, 2008. Uncertainty analysis in cfd verification and validation methodology and procedures. Recommended Procedures and Guidelines, 7.5-03-01-01, Rev 02 URL: https://ittc.info/media/4184/75-03-01-01.pdf.
[8] Korkmaz, K., Werner, S., Bensow, R., 2019. Numerical friction lines for cfd based form factor determination. VIII International Conference on Computational Methods in Marine Engineering Conference Paper.
[9] Korkmaz, K., Werner, S., Bensow, R., 2022. Scaling of wetted-transom resistance for improved full-scale ship performance predictions. Elsevier, Ocean Engineering 226. URL: https://doi.org/10.1016/j.oceaneng.2022.112590.
[10] Korkmaz, K.,Werner, S., Sakamoto, N., Queutey, P., Deng, G., Yuling, G., Guoxiang, D., Maki, K., Y.H., Akinturk, A., Sayeed, T., Hino, T.and Zhao, F., Tezdogan, T., Demirel, Y., Bensow, R., 2021. Cfd-based

form factor determination method. Elsevier, Ocean Engineering 220. URL: https://doi.org/10.1016/j.oceaneng.2020.108451.
[11] Larsson, L., Raven, C., H., 2010. Ship and resistance flow. SNAME, USA, Principles of Naval Architecture Series ISBN 978-0-939773-76-3.
[12] Larsson, L., Stern, F., Visonneua, M., 2010. Gothenburg 2010: AWorkshop on Numerical Ship Hydrodynamics. Proceedings, Volume II. Report No. R-10:122, ISSN No. 1652-9189.
[13] Mikkelsen, H., Steffensen, L., Ciortan, C., Walther, J.H., 2019. Ship scale validation of cfd model of selfpropelled ship. In R. Bensow, J. Ringsberg (Eds.), MARINE 2019 Computational Methods in Marine Engineering VIII. International Center for Numerical Methods in Engineering.
[14] Prohaska, C., 1966. A simple method for the evaluation of the form factor and low speed wave resistance. Proceeding of 11th ITTC .
[15] Quintuña, M., Horn, P., Zhang, J., Sprenger, F., 2024. Combined efd and cfd approach for full scale ship resistance predictions using the form factor. The American Society of Mechanical Engineers https://doi.org/10.1115/OMAE2024-126397.
[16] STAR-CCM+, S., 2023. Siemens software. URL: https://plm.sw.siemens.com/en-US/simcenter/fluids-thermal-simulation/star-ccm/.
[17] Stern, F.,Wilson, R., Coleman, H., Paterson, E., 2021. Comprehensive approach to verification and validation of cfd simulations—part 1: Methodology and procedures. J. Fluids Eng. 2001, 123, 793–802. and ITTC 75-03-01-01 Rev 04 Recommended Procedures and Guidelines Uncertainty Analysis. ITTC: Zürich, Switzerland.
[18] Watanabe, K., 1973. Note to the performance committee URL: https://ittc.info/media/3267/rpec.pdf.
[19] Wilson, R., Stern, F., , Coleman, H., Paterson, E., 2001. Comprehensive approach to verification and validation of cfd simulations—part 2: Application for rans simulation of a cargo/container ship. J. Fluids Eng. 2001, 123, 803–810 .
[20] Yao, J., X., Liu, Z., Song, X., Su, Y., 2021. Ship maneuvering prediction with hydrodynamic derivatives from rans: Development and application. Ocean Engineering 231, 109036. URL: https://doi.org/10.1016/j.oceaneng.2021.109036.